CrossMark

Glass transition kinetics and thermal stability of $Se_{82-x}Te_{18}Sb_x$ (x = 0, 4, 8 and 12 at %) glassy alloys

Vandita Rao[1] · D. K. Dwivedi[1]

Abstract Glass transition kinetics of $Se_{82-x}Te_{18}Sb_x$ (x = 0, 4, 8 and 12 at.%) glassy alloys has been studied using differential scanning calorimetry (DSC). DSC runs were taken at different heating rates (5, 10, 15 and 20 K/ min) for each samples. Heating rate dependence of glass transition temperature (T_g) has been studied using Lasocka empirical relation. Activation energy of glass transition (E_g) has been determined using Kissinger and Moynihan's relation. Effect of Sb concentration on glass transition temperature and activation energy has been studied. Thermal stability of $Se_{82-x}Te_{18}Sb_x$ glassy alloys has also been investigated using Dietzal relation, Saad and Poulin relation, Hurby parameter (H_r) and Lie and Liu parameter (γ). Compositional dependence of parameters investigated for thermal stability has also been studied.

1 Introduction

Semiconductor chalcogenide glasses have received much attention in the recent past due to their useful applications in modern electronics, optoelectronics, integrated optics, solar cells, optical memory devices, optical recording systems, chemical and biosensors [1–10].

Se-based chalcogenide glasses have high transparency in broad middle and for IR regions along with strong non-linear properties. Besides this amorphous selenium has got tremendous potential in xeroxing applications.

Also Se based glasses have low thermal conductivity, low melting point and unexpected stability which allows them to be used for glass formation while doping with various other elements [11, 12]. Tellurium on the other hand posses properties required in cutting edge technologies based on chalcogenide glasses [13]. These properties are related to ultrafast crystallization used in phase change optical data storage devices [14–17] and transmittance in the for IR regions used in IR optics and optical fiber [18, 19]. Though Se based chalcogenide glasses have got a good number of applications in variety of domains, however, they suffer from thermal in stability leading to crystallization which happens to be one of the drawback of these alloys. Se–Te alloys are found to be useful from technological point of view only when these alloys are thermally stable with respect to time and temperature when they are in use. Many researchers have made attempt to improve the stability of Se–Te alloy by adding a third element such as (Ge, Bi, Zn, Sb, In etc). Alloying gives smaller aging effect, higher sensitivity and higher crystallization temperature [20–23]. We have chosen Sb as an additive element in Se–Te alloy may expand the glass forming area and also can create compositional and configurationally disordered system with respect to binary alloy which will be useful in understanding the glass transition kinetics and thermal stability of Se–Te–Sb system. Also addition of Sb impurity to Se–Te system increases the electrical conduction and thermal stability of the material [24].

It has been further reported that the glass transition temperature (T_g) is found to be increasing with Sb content which clearly indicates that there is a cross linking of Se–Te chains after doping with Sb [25].Optical and electrical properties of Se–Te-Sb system has been studied extensively by other workers [26–31], but very little attention

✉ D. K. Dwivedi
  todkdwivedi@gmail.com

[1] Amorphous Semiconductor Research Lab, Department of Applied Science, Madan Mohan Malaviya University of Technology, Gorakhpur 273010, India

has been paid on glass transition and crystallization kinetics of Se–Te–Sb glassy alloys.

From ongoing discussions, we find that glass transition, glass stability and chemical stability are the prominent properties of glassy materials to be used in various phase change recording media.

The present work is concerned with the study of glass transition kinetics and thermal stability of $Se_{82-x}Te_{18}Sb_x$ (x = 0, 4, 8 and 12 at.%) glassy alloys. Sb has been added as a chemical modifier on the cost of Se. Calorimetric studies has been carried out under non-isothermal conditions at different heating rates. Activation energy of glass transition has been analysed. Effect of Sb additive on glass transition mechanism and activation energy has been reported. Thermal stability has also been examined using different parameters.

2 Experimental

Glassy alloys $Se_{82-x}Te_{18}Sb_x$ (x = 0, 4, 8 and 12 at.%) was prepared by the most frequently used melt quenching technique. An appropriate amount of high purity (99.999 pure) Se, Te and Sb were weighed accordance to their atomic percentage by using an electronic balance(LIBROR, AEG-120) with the least count of 10^{-4} g and placed into ultra-cleaned quartz ampoules (length 5 cm and diameter 8 mm). To avoid oxidation the ampoules were evacuated and sealed under a vacuum of 10^{-4} Torr. Each ampoule was kept inside the furnace at an appropriate temperature (above the melting point of each constituents). The temperature was raised at a rate of 3–4 °C/ min. The temperature was kept at 1000 K for 24 h. During the heating process, the ampoules were constantly rocked by rotating ceramic rod to ensure the homogeneity of alloying materials. The ampoules with molten materials were rapidly quenched into ice-cooled water. The rapid cooling was done to convert the melt in highly viscous liquids i.e. in glassy form. The ingots of glassy materials were taken out from ampoules by breaking them. Prepared glassy material were grind to make fine powder for DSC studies.

10–20 mg of each sample was heated at a constant heating rate and changes in heating flow with respect to an empty pan were measured by using differential scanning calorimetry (Shimazadu, Japan Model 60).

3 Theoretical basis

The understanding of glass transition kinetics is one of the most important problems in the area of glasses. This can be studied in terms of glass transition temperature (T_g) and activation energy of glass transition (E_g). The evaluation of

E_g using the theory of structural relaxation as developed by Moynihan and other workers [32–34] from the heating rate dependence of glass transition temperature is widely used in the literature. Kissinger's method [35], which was originally derived for the determination of activation energy of crystallization, can be used for evaluation of activation energy of the glass transition process in chalcogenide glasses too [36]. We have, therefore, used both Kissinger's method and Moynihan's method for evaluation of the activation energy of structural relaxation in chalcogenide glasses. The theoretical basis of both methods is given below.

3.1 Moynihan's method

The heating rate dependence of the glass transition temperature in chalcogenide glasses is interpreted by Moynihan et al. in terms of thermal relaxation phenomenon. In this kinetic interpretation, the enthalpy at a particular temperature and time H(T, t) of the glassy system, after an instantaneous isobaric change in temperature, relaxes isothermally toward a new equilibrium value $H_c(T)$. The relaxation equation can be written in the following form [32]

$$\left(\frac{\partial H}{\partial t}\right) = -\frac{(H - H_c)}{\tau}, \tag{1}$$

where τ is a temperature-dependent structural relaxation time and is given by the following relation:

$$\tau = \tau_o \exp\left(-\frac{E_g}{RT}\right) \exp\left[-c(H - H_c)\right], \tag{2}$$

where τ_o and c are constants and E_g is the activation energy of relaxation time. Using the above equations, it can be shown [33, 34] that

$$\frac{d(\ln \beta)}{d(1/T_g)} = -\frac{E_g}{R} \tag{3}$$

From Eq. (3) it is evident that $\ln\beta$ versus $1/T_g$ plot should be straight line and activation energy involved in the molecular motions and rearrangement around T_g can be calculated from the slope of this plot.

3.2 Kissinger's method

This method is commonly used in analyzing crystallization data in DSC. During the isothermal transformation, the extent of crystallization (α) of a certain material is represented by Avrami's equation [37, 38]

$$\alpha(t) = 1 - \exp\left[-(Kt)^n\right], \tag{4}$$

where 'K' is the rate constant and 'n' is the order parameter that depends upon the mechanism of crystal growth.

The rate constant K is given by the Arrhenius equation

$$K = K_o \exp\left(\frac{-E_c}{RT}\right) \tag{5}$$

According to Kissinger, Eq. (4) can be approximated as

$$\left(\frac{d\alpha}{dt}\right) = nK^n t^{n-1}(1-\alpha) \tag{6}$$

Expressing t in terms of α from Eq. (4), the crystallization rate ($d\alpha/dt$) becomes

$$\left(\frac{d\alpha}{dt}\right) = AnK(1-\alpha), \tag{7}$$

where $A = [-\ln(1-\alpha)]^{(n-1)/n}$.

In non-isothermal crystallization, it is assumed that there is a constant heating rate in the experiment. The relation between the sample temperature T and heating rate β can be written in the form:

$$T = T_i + \beta t, \tag{8}$$

where T_i is the initial temperature.

The derivative of K with respect to time can be obtained from Eqs. (5) and (8) as follows:

$$\frac{dK}{dt} = \left(\frac{dK}{dT}\right)\left(\frac{dT}{dt}\right) = \left(\frac{\beta E_c}{RT_c}\right)K \tag{9}$$

Using Eqs. (7) and (9), we have

$$\ln\left(\frac{\beta}{T_c^2}\right) = \left(\frac{-E_c}{RT_c}\right) + \text{constant}, \tag{10}$$

where T_c is the crystallization temperature.

Although originally derived for the crystallization process, it has been found that this relation is also valid for the glass transition process [36] and hence the above equation reduces to the following form for glass transition kinetics.

$$\ln\left(\frac{\beta}{T_g^2}\right) = \left(\frac{-E_g}{RT_g}\right) + \text{constant} \tag{11}$$

Variations of $\ln(\beta/T_g^2)$ versus $1000/T_g$ were plotted and activation energy of glass transition (E_g) has been calculated from the slope of these plots.

4 Results and discussion

4.1 DSC curve

Glass transition phenomena can be conveniently observed by differential scanning calorimetry (DSC). DSC is able to measure the amount of energy absorbed or released during transition. Glass transition occurs as the temperature of an amorphous solid is increased and characterized by a decrease in viscosity. This transition is an endothermic process and appears, at the glass transition temperature as a small dip of the DSC curve [39]. The DSC curves, for the glassy alloys $Se_{82-x}Te_{18}Sb_x$ (x = 0, 4, 8 and 12 at.%) were recorded at four heating rates of 5, 10, 15 and 20 K/min. Figure 1a–d show the typical DSC thermogram for $Se_{82-x}Te_{18}Sb_x$ (x = 0, 4, 8 and 12 at.%) at heating rate 20 K/min. It is clear from these figures that well-defined endothermic peaks are observed at the glass transition temperature (T_g). Similar DSC curves were observed for other compositions at heating rates 5, 10 and 15 K/min. Single glass transition has been observed for the studied compositions (x = 0, 4, 8 and 12 at.%). This implies that all four studied compositions are homogeneous.

4.2 Glass transition temperature (T_g)

Endothermic peak corresponds to the glass transition phenomenon which is represented by the glass transition temperature (T_g). T_g has been defined as the temperature which corresponds to the intersection of two linear portions adjoining the transition elbow of the DSC traces in the endothermic direction [3]. The values of glass transition temperature for present glassy alloys at different heating rates are given in Table 1.

As evident from this table, it is observed that the characteristic glass transition temperature shifts towards the higher values as the heating rate increases from 5 to 20 K/min. In addition, T_g increases with an increase in Sb content at the same heating rate. Variation of T_g with Sb content in $Se_{82-x}Te_{18}Sb_x$ (x = 0, 4, 8 and 12 at.%) glassy alloy is shown in Fig. 2.

The Sb atom has a larger atomic/ionic radius than Se and Te atoms. Thus, when Sb is added to the Se–Te lattice, the lattice distorts due to the disturbed Vander Waal type forces between chains and the rings of the chalcogen atoms. The distortion in the lattice gives rise to more three-dimensional disorder in the material. It seems therefore that introduction of Sb in Se–Te system introduces some structural changes. The increase of T_g with initial addition of Sb could be accounted for by cross linking in the chains which increases the chain length thereby enhancing T_g.

4.3 Dependence of glass transition temperature on heating rate

The glass transition temperature T_g represents the strength or rigidity of the glassy structure of the alloys. It is well known that glass transition temperature T_g of glassy alloys varies with the heating rate β [40–44]. Firstly, Lasocka
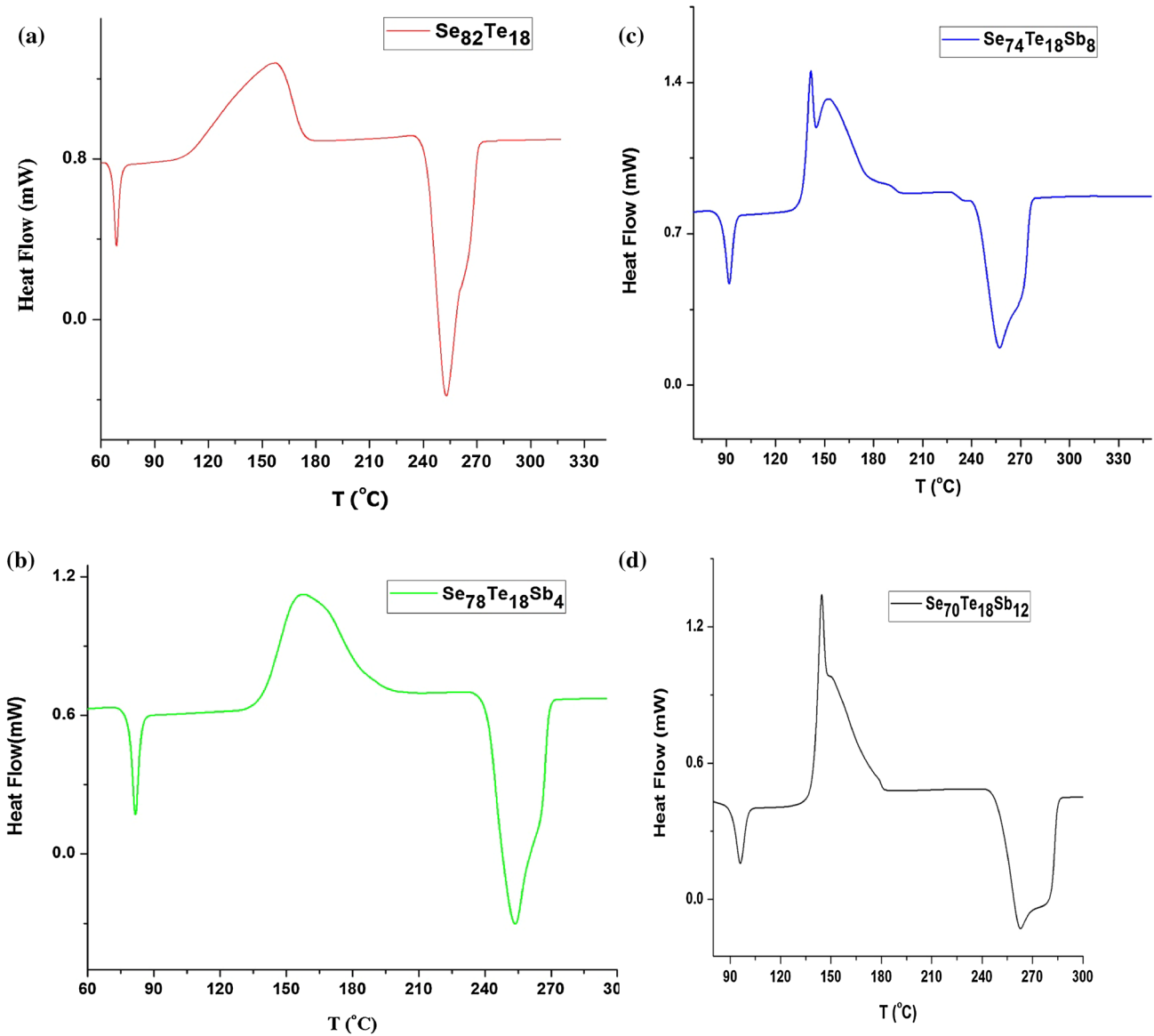
Fig. 1 DSC scans taken at heating rate 20 K/min for $Se_{82-x}Te_{18}Sb_x$ glassy alloys. **a** x = 0, **b** x = 4, **c** x = 8, **d** x = 12

Table 1 The values of glass transition temperature (T_g) in K for $Se_{82-x}Te_{18}Sb_x$ (x = 0, 4, 8 and 12 at.%) glassy alloys at different heating rates.

Heating rate (K/min)	Glass transition temperature (T_g) for different samples			
	$Se_{82}Te_{18}$	$Se_{78}Te_{18}Sb_4$	$Se_{74}Te_{18}Sb_8$	$Se_{70}Te_{18}Sb_{12}$
5	336	348	357	361
10	339	351	361	365
15	341	353	363	368
20	343	355	369	370

studied the effect of heating rate on glass transition temperature T_g of splat cooled $Te_{85}Ge_{15}$. Lasocka measured the T_g of Te–Ge alloy over a wide range of heating rate β from 1.25 to 80°/min. The results are described by a linear plot [45].

$$T_g = A + Blog\beta \tag{12}$$

where A and B are constants for a given glassy composition (A = 386 K and B = 14.88 for $Te_{85}Ge_{15}$ glassy alloy). Since the function $T_g(log \beta)$ is linear, it was possible to obtain the exact $T_g = A$ value by extrapolation of the data to β = 1. Depending on β, various configurational states of the metastable melt are obtained upon heating of glass in the DSC experiments. Thus, the nature of the function $T_g(log \beta)$ may
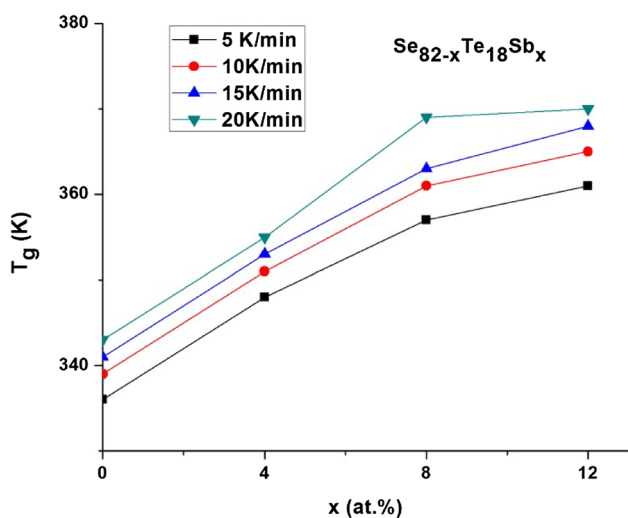
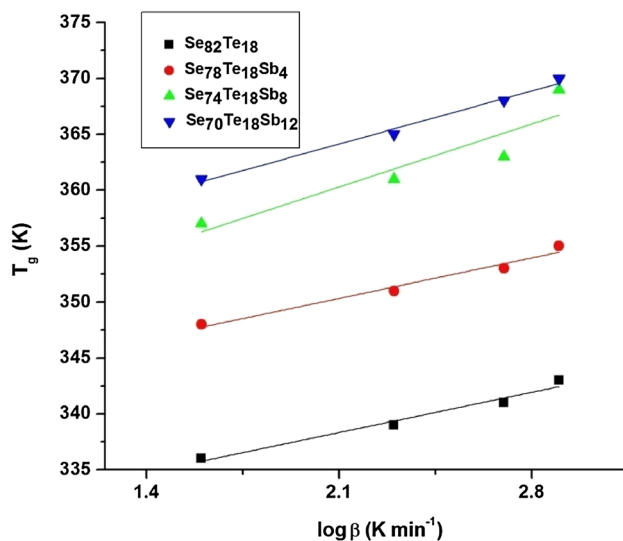**Fig. 2** Variation of glass transition temperature (T_g) with composition in $Se_{82-x}Te_{18}Sb_x$ glassy alloys

Table 2 Kinetic parameters 'A' and 'B' for $Se_{82-x}Te_{18}Sb_x$ glassy alloys

Samples	A	B
$Se_{82}Te_{18}$	327.54	5.13
$Se_{78}Te_{18}Sb_4$	339.54	4.13
$Se_{74}Te_{18}Sb_8$	343.37	6.05
$Se_{70}Te_{18}Sb_{12}$	349.88	6.78

Fig. 4 Variation of kinetic parameter B with composition in $Se_{82-x}Te_{18}Sb_x$ glassy alloys

Fig. 3 Plot of T_g versus log β for glassy $Se_{82-x}Te_{18}Sb_X$ glassy alloys

lower the value of B, the lower the cooling rate of the melt. The physical significance of B seems to be related with the response of the configurational changes within the glass transformation region.

From Table 2, it is clear that the values of A are in good agreement with the experimental data. The different values of B obtained in Table 2 clearly indicate that all alloys undergo different structural changes. Variation of kinetic parameters B with composition in $Se_{82-x}Te_{18}Sb_x$ glassy alloys is shown in Fig. 4.

4.4 Evaluation of activation energy (E_g) for glass transition

Using Moynihan's relation (see Eq. 3), the variations of lnβ against $1000/T_g$ were plotted for $Se_{82-x}Te_{18}Sb_x$ (x = 0, 4, 8 and 12 at.%) glassy alloys. These plots are shown in Fig. 5. The slope of these plots was used to calculate the activation energy of glass transition process. The evaluated values of activation energies (E_g) using Eq. 3 is listed in Table 3.

The values of E_g are also evaluated using Kissinger's method (see Eq. 11) from the slopes of plots of $\ln(\beta/T_g^2)$
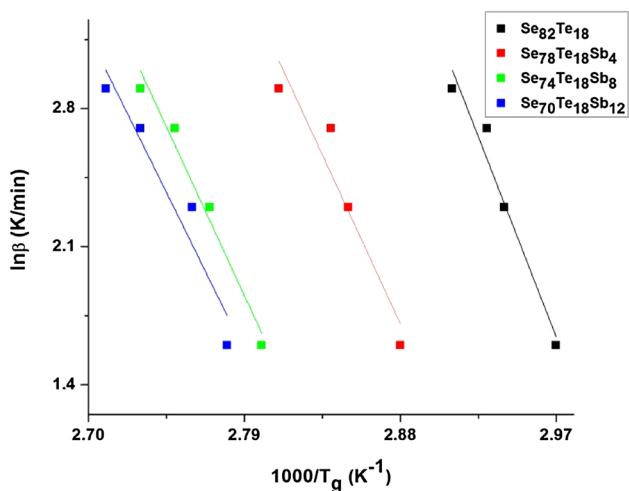
elucidate somewhat the rate-dependence of the configurational changes, or to some extent give information on the kinetics of the glass to supercooled-liquid transition.

The above empirical relation (Eq. 12) has been applied in the present paper to study the heating rate dependence of glass transition temperature (T_g) of Se–Te–Sb glassy alloys.

The plot of T_g versus log β for the $Se_{82-x}Te_{18}Sb_x$ (x = 0, 4, 8 and 12 at.%) glassy alloys is shown in Fig. 3. From the linear relationship, the values of A and B are deduced and listed in Table 2.

The value of A indicates the glass transition temperature (T_g) for a heating rate of 1 K/min. The values of B depends on the cooling rate during the preparation of the glass, the

Fig. 5 Variation of lnβ versus $1000/T_g$ for $Se_{82-x}Te_{18}Sb_x$ glassy alloys

Table 3 The values of activation energy of glass transition (E_g) for $Se_{82-x}Te_{18}Sb_x$ (x = 0, 4, 8 and 12 at.%) glassy alloys

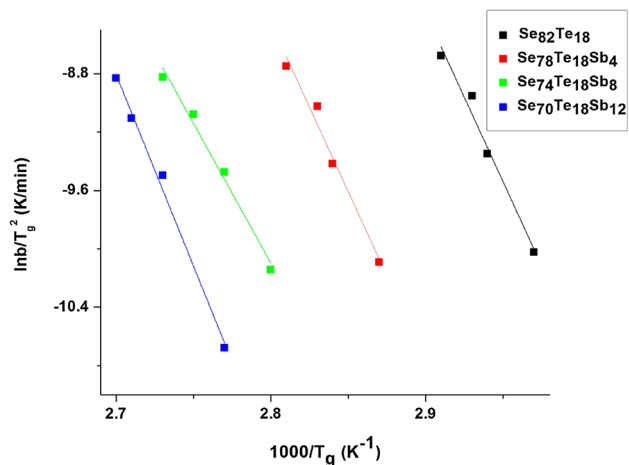| Samples	E_g (kJ/mole)	
	Kissinger method	Moynihan method
$Se_{82}Te_{18}$	163.72	161.45
$Se_{78}Te_{18}Sb_4$	187.53	184.49
$Se_{74}Te_{18}Sb_8$	188.60	190.69
$Se_{70}Te_{18}Sb_{12}$	205.36	201.32

Fig. 6 Variation of $lnβ/T_g^2$ versus $1000/T_g$ for $Se_{82-x}Te_{18}Sb_x$ glassy alloys

against $1000/T_g$ for various glassy systems. The plots of $ln(β/T_g^2)$ versus $1000/T_g$ are also shown in Fig. 6 for $Se_{82-x}Te_{18}Sb_x$ (x = 0, 4, 8 and 12 at.%) glassy alloys. These values are also given in Table 3. It is clear from Table 3 that E_g values obtained from Kissinger's method are in
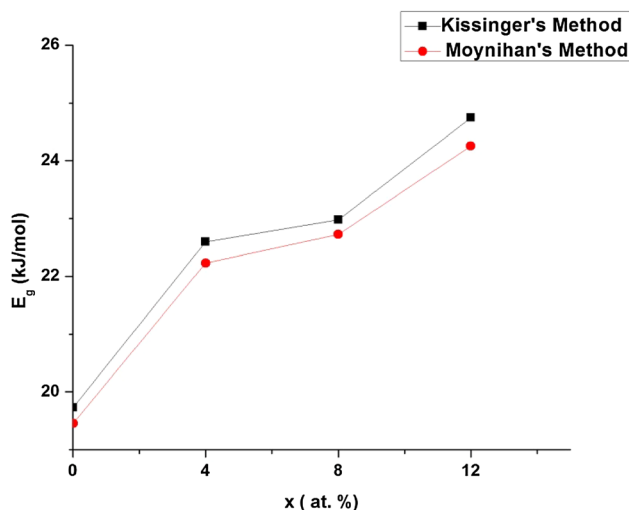

Fig. 7 Compositional dependence of activation energy of glass transition (E_g)

good agreement with the E_g values obtained using Moynihan's method. This means that one can use any of the two equations (Eqs. 3, 11) to calculate the activation energy of the glass transition.

4.5 Composition dependence of the activation energy of the glass transition (E_g)

The composition dependence of the activation energy of the glass transition is shown in Fig. 7. From Fig. 7, it is clear that the value of E_g is minimum for binary composition. In ternary glassy alloys E_g is minimum for 4 at.% of Sb and the increasing sequence of E_g is $(E_g)_{x=4} < (E_g)_{x=8} < (E_g)_{x=12}$. The increase in E_g due to addition of Sb in binary Se–Te system can be explained in terms of average heat of atomization (H_S) for these alloys. The average heat of atomization, H_S, is based on chemical bonding aspects which is defined for a binary alloy X_aY_b as a direct measure of cohesive energy, i.e., of the average bond strength. H_S can be given as:

$$H_S = \frac{[a(H_S)_X + b(H_S)_Y]}{(a+b)} \tag{13}$$

For a ternary alloy $X_aY_bZ_c$, it can be expressed as:

$$H_S = \frac{[a(H_S)_X + b(H_S)_Y + c(H_S)_Z]}{(a+b+c)} \tag{14}$$

where $(H_S)_X$, $(H_S)_Y$, $(H_S)_Z$ are the heat of atomization of atoms X, Y and Z respectively. The H_S values of Se, Te and Sb are 227, 197 and 262 kJ/mol respectively. The value of H_S for binary alloy $Se_{82}Te_{18}$ and ternary

Table 4 The average bond strength of ternary $Se_{82-x}Te_{18}Sb_x$ (x = 0, 4, 8 and 12 at.%) glassy alloys

Sample	H_S (kJ/mol)
$Se_{82}Te_{18}$	221.60
$Se_{78}Te_{18}Sb_4$	223.00
$Se_{74}Te_{18}Sb_8$	224.40
$Se_{70}Te_{18}Sb_{12}$	225.80

Table 5 The thermal stability parameter ΔT, S, Hruby parameter H_r, and parameter γ for $Se_{82-x}Te_{18}Sb_x$ (x = 0, 4, 8 and 12 at.%) glassy alloys

Sample	$\Delta T(K)$	S	H_r	γ
$Se_{82}Te_{18}$	86	12.78	0.89	0.49
$Se_{78}Te_{18}Sb_4$	62	9.20	0.56	0.47
$Se_{74}Te_{18}Sb_8$	51	5.25	0.47	0.44
$Se_{70}Te_{18}Sb_{12}$	62	6.10	0.53	0.48

alloys $Se_{82-x}Te_{18}Sb_x$ (x = 0, 4, 8 and 12 at.%) are given in Table 4. From this table, it is clear that the value of H_S is larger for ternary alloys as compared to that of binary alloy. This explains the higher values of E_g for ternary alloys as compared to that of binary $Se_{82}Te_{18}$ alloy.

5 Thermal stability and glass forming ability

Various quantitative methods are suggested to evaluate the level of stability of the glassy alloys. The glass transition temperature affords valuable information on the properties of many materials for example, on their glass forming ability, thermal stability of the glassy state, and even on the kinetics of crystal growth. Glass formation is essentially a kinetic process, it is favored when the melt can be significantly under cooled to low enough temperatures so that the viscosity of the under cooled melt is high and consequently it gets frozen into the glassy state. The first stability criterion was introduced by Dietzal [46]. This approach investigates the difference between T_c and T_g as $\Delta T = (T_c - T_g)$ which is used as criterion to decide the thermal stability in the glasses. The problem with the ΔT parameter is that it considers only the stability of the glassy phase against crystallization and not the ease of glass formation [47]. A large ΔT value may indicate that the under cooled liquid can remain stable in a wide temperature range without crystallization, thus leading to a larger GFA of the alloy.

Hruby proposed a method which allows fast evaluation of glass-forming tendency based on relative position of the recrystallization, transformation and melting temperatures. These temperatures are determined by means of DSC. One assumes that the glass-forming tendency is

proportional to the thermal stability of glass. The glass-forming tendency is expressed numerically, thus enabling one to compare different kinds of glasses and the influence of various impurities. The validity of the model is experimentally verified on various systems [48–51].

Hruby [52] has introduced a parameter H_r, which combines both nucleation and growth aspects of phase transformation, as an indicator of GFA, and is given by

$$H_r = \frac{(T_c - T_g)}{(T_m - T_c)}, \tag{15}$$

where T_m is the melting temperature. A higher value of $(T_c - T_g)$ delays the nucleation process and the small value of $(T_m - T_c)$ retards the growth process. If $H_r \leq 0.1$ the glass is usually difficult to prepare. Good glass former has values of $H_r \geq 0.4$ [53].

Saad and Poulin [54] have looked for simple elements allowing stability evaluation. The comparison between DSC scans showed that, among other features, more stable glasses show broader exotherms. Since DSC scans are carried out at a constant heating rate, therefore peak width is directly related to the time necessary for crystallization. As this width is not always easy to measure on real curves, so they have chosen to consider the difference $(T_c - T_g)$ between the temperature of the maximum of the exotherm and the crystallization onset. Finally, the new criterion appeared as

$$S = \frac{(T_c - T_g)(T_p - T_c)}{T_g}, \tag{16}$$

where T_p is the peak crystallization temperature.

Lu and Liu [55, 56] has proposed a conceptual approach to evaluate glass-forming ability for various glass-forming systems has been proposed from a physical metallurgy point of view. It was found that the glass-forming ability for non-crystalline materials was related mainly to two factors, i.e., $1/(T_g + T_m)$ and T_c (where T_c is the onset crystallization temperature, T_g the glass transition temperature, and T_m the melting temperature), and could be estimated by a unified parameter γ given as

$$\gamma = \frac{T_c}{T_g + T_m} \tag{17}$$

Lie and Liu method has been confirmed and validated by experimental data in various glass-forming systems. The ideal value is found to be equal to 0.5 for γ parameter. The obtained result for the prepared glassy alloys shows that studied compositions have good glass forming ability. Various thermal stability parameters have been estimated for $Se_{82-x}Te_{18}Sb_x$ glassy alloys and listed in Table 4.

From Table 5, it is clear that all thermal stability parameters decrease with an increasing content of Sb in $Se_{82-x}Te_{18}Sb_x$ glassy alloys. It indicates that maximum values of various parameters of thermal stability are observed for 4 at.% of Sb.

6 Conclusion

Se–Te–Sb glassy alloy has been prepared using melt quench technique. Glass transition kinetics and thermal stability of $Se_{82-x}Te_{18}Sb_x$ (x = 0, 4, 8 and 12 at.%) glassy alloys have been studied using DSC technique. The major conclusions are:

1. Glass transition temperature (T_g) increases with increase in concentration of Sb in Se–Te matrix which may be attributed to the fact that addition of Sb results into cross –linking the chains which increase the chain length which is responsible for enhancement of T_g.
2. Activation energy of glass transition (E_g) has been evaluated using Kissinger and Moynihan relations. The activation energy (E_g) increases with Sb content. The higher value of E_g for ternary alloys as compared to that of binary $Se_{82}Te_{18}$ alloy is explained in terms of average heat of atomization for these alloys.
3. Thermal stability parameters ΔT, S, H_r and γ decreases with increase in concentration of Sb in $Se_{82-x}Te_{18}Sb_x$ (x = 0, 4, 8 and 12 at.%) glassy alloys. It has been observed that among ternary compositions $Se_{82}Te_{18}Sb_4$ is more thermally stable.

Thus, from studied all $Se_{82-x}Te_{18}Sb_x$ (x = 0, 4, 8 and 12 at.%) glassy alloys the optimum composition for phase change optoelectronic applications is found in $Se_{78}Te_{18}Sb_4$.

References

1. T. Ohta, J. Optoelectron. Adv. Mater. **3**, 609 (2001)
2. S. Kumar, K. Singh, Physica B **406**, 1519 (2011)
3. O.A. Lafi, J. Alloys Compd. **519**, 123 (2012)
4. G.F. Zhou, Mater. Sci. Eng. A **304–306**, 73 (2001)
5. N. Tanwar, V.K. Saraswat, J. Non-Cryst. Solids **394–395**, 1 (2014)
6. M.A. Abdel-Rahim, M.M. Hafiz, A.Z. Mahmoud, Prog. Nat. Sci. **25**, 169 (2015)
7. M.A. Abdel-Rahim, M.M. Hafiz, A.Z. Mahmoud, Phase Transit. (2016). doi:10.1080/01411594.2015.1136912
8. D.K. Dwivedi, N. Shukla, H.P. Pathak, V. Rao, Chalcogenide Lett. **13**(4), 177 (2016)
9. D.K. Dwivedi, N. Shukla, N. Mehta, Electron. Lett. (2016). doi:10.1049/el.2016.1798
10. D.K. Dwivedi, N. Shukla, N. Mehta, Mater. Sci. Mater. Electron. (2016). doi:10.1007/s10854-016-5352-1
11. Y. Sung-Min, L. Nam-Yeal, R. Sang-Ouk, C. Kyu-Jeong, Y.S. Park, L. Seung-Yun, Y. Byoung-Gon, K. Myung-Jin, C. Se-Young, M. Wuttig, IEEE Electron. Device Lett. **27**, 445 (2006)
12. Y. Lu, S. Song, X. Shen, L. Wu, Z. Song, B. Liu, S. Dai, Q. Nie, ECS Solid State Lett. **2**(10), 94 (2013)
13. R. Svoboda, M. Kincl, J. Malek, J. Alloys Compd. **644**, 40 (2015)
14. S. Raoux, W. Welnic, D. Ielmini, Chem. Rev. **110**, 240 (2010)
15. M. Wuttig, C. Steimer, Appl. Phys. A **87**, 411 (2007)
16. M. Wuttig, N. Yamada, Nat. Mater. **87**, 824 (2007)
17. W. Welnic, J.A. Kalb, D. Wamwangi, J. Mater. Res. **22**, 2368 (2007)
18. A. Zakery , S.R. Elliott. J. Non-Cryst. Solids **330**, 1 (2003)
19. A.A. Wilhelm, C. Boussard-Pledel, Q. Coulombier, J. Lucas, B. Bureau, P. Lucas, Adv. Mater. **19**, 3796 (2007)
20. M.A. Abdel-Rahim, A. Gaber, A.A. Abu- Sehly, N.M. Abdela-zim, J. Non-Cryst. Solids **376**, 158 (2013)
21. M.A. Abdel-Rahim, J. Non-Cryst. Solids **241**, 121 (1998)
22. R. Chander, R. Thangaraj, Thin Solid Films **520**, 1757 (2012)
23. J.M. Saiter, J. Ledru, A. Hamou, G. Saffarini, Physica B **245**, 256 (1998)
24. H.P. Pathak, N. Shukla, V. Kumar, D.K. Dwivedi, Opt. Mater. **52**, 69 (2016)
25. S.K. Tripathi, V. Sharma, A. Thakur, J. Non-Cryst. Solids **351**, 2468 (2005)
26. N.S. Saxena, J. Non-Cryst. Solids **345–346**, 161 (2004)
27. M.A. Abdel-Rahim, A.Y. Abdel-Latif, A.S. Soltan, Physica B **291**, 41 (2000)
28. D.K. Dwivedi, H.P. Pathak, R.K. Shukla, A. Kumar, Am. J. Mater. Sci. Eng. **1**(3), 46 (2013)
29. D.K. Dwivedi, H.P. Pathak, N. Shukla, A. Kumar, J. Ovonic Res. **10**, 15 (2014)
30. D.K. Dwivedi, H.P. Pathak, R.K. Shukla, A. Kumar, Int. J. Light Electron. Opt. **126**(6), 635 (2015)
31. D.K. Dwivedi, H.P. Pathak, N. Shukla, V. Kumar, Adv. Sci. Lett. **20**(5–6), 1081 (2014)
32. S.O. Kasap, C. Juhaz, J. Mater. Sci. **21**, 1329 (1986)
33. J.P. Larmagnac, J. Grenet, P. Michon, J. Non-Cryst. Solids **45**, 157 (1981)
34. C.T. Moynihan, A.J. Easteal, J. Wilder, J. Tucker, J. Phys. Chem. **78**, 2673 (1974)
35. H.E. Kissinger, Anal. Chem. **29**, 1702 (1957)
36. N. Mehta, A. Kumar, J. Optoelectron. Adv. Mater. **7**, 1473 (2005)
37. M. Avrami, J. Phys. Chem. **7**, 1103 (1939)
38. M. Avrami, J. Phys. Chem. **8**, 212 (1940)
39. F. Perkin, Elmer User Manual, T Series/Unix DSC, Norwalk (1995)
40. G.C. Das, M.B. Bever, D.R. Uhlmann, J. Non-Cryst. Solids **7**, 251 (1972)
41. M.K. El-Mously, M.M. El-Zaidia, J. Non-Cryst. Solids **27**, 265 (1978)
42. M.A. Abkovitz, in *The Physics of Se and Te*, ed. E. Gerlach and P. Grosse (Springer, Berlin, 1978), p. 178
43. M.F. Kotkata, M.K. El-Mously, Acta Phys. Hung. **54**, 303 (1983)
44. K. Weiser, R.J. Gambino, J.A. Reinhold, Appl. Phys. Lett. **22**, 48 (1973)
45. M. Lasocka, Mater. Sci. Eng. **23**, 173 (1976)
46. A. Dietzel, Glasstech. Ber. **22**, 41 (1968)
47. C. Suryanarayana, I. Seki, A. Inoue, J. Non-Cryst. Solids **355**, 355 (2009)

48. V. Nidhi, V. Modgil, V.S. Rangra, J. Therm. Anal. Calorim. (2015). doi:10.1007/s10973-015-4621-1
49. M.A. Abdel-Rahim, A. Gaber, A.A. Abu-Sehly, N.M. Abdela-zim, Thermochim. Acta **566**, 274 (2013)
50. F.A. Wahab, Physica B **406**, 1053 (2011)
51. N. Sharma, S. Sharda, V. Sharma, P. Sharma, J. Non-Cryst. Solids **371–372**, 1 (2013)
52. A. Hruby, J. Czech. Phys. B **22**, 1187 (1972)
53. M. Saad, M. Poulin, Mater. Sci. Forum **19–20**, 11 (1987)
54. Y. Calventus, S. Surinach, M.D. Baro, Mater. Sci. Eng. **226–228**, 88 (1997)
55. Z.P. Lu, C.T. Liu, Phys. Rev. Lett. **91**, 115505–115505 (2003)
56. E.S. Park, D.H. Kim, W.T. Kim, J. Appl. Phys. **86**, 061907–061903 (2005)